

Numerical Study of One-Phase Stefan-Type Problems

Seyed Shojaeddin Pishnamaz Mohammadi¹ and Karim Ivaz^{1*}

¹Department of Applied Mathematics, University of Tabriz, Iran

Keywords:

Stefan problem,
Non-classical heat equation,
Numerical method,
Convective boundary condition,
Error analysis

AMS Subject Classification (2020):

80A22; 65M06; 65M15

Article History:

Received: 22 August 2024,
Accepted: 5 February 2025

Abstract

We all know that parabolic equations with non-classical boundary conditions and Stefan's problem have become very popular in recent years due to their many applications in more basic and applied science problems. Also, differential equations with integral conditions have found wide applications in solving chemistry and physics problems. Many problems that appear in heat transfer can be reduced to non-classical problems with integral conditions. In this document, we first mention the application of Stefan's one-phase problems, including the non-classical thermal equation and the integral boundary condition, in problems related to chemistry. Then we examine a numerical technique to solve it and prove the convergence of the method. Finally, numerical examples are presented to demonstrate the effectiveness of the method for solving linear and non-linear diffusion-response equations with these non-classical conditions.

© 2025 University of Kashan Press. All rights reserved.

1 Introduction

The Stefan problem in chemistry typically refers to a class of problems involving phase changes, such as the melting of ice or the solidification of a liquid. These problems are named after Josef Stefan, an Austrian physicist, and they generally involve solving the heat equation with a moving boundary. The Stefan problem has several important applications in chemistry and related fields, particularly in processes involving phase transitions. Here are some key applications:

- Crystal Growth:** In the manufacturing of semiconductors and other crystalline materials, controlling the rate and uniformity of crystal growth is crucial. The moving border among the liquid and solid phases of the material being crystallized can be modeled using the Stefan problem to predict how temperature gradients and cooling rates affect the growth.
- Freezing and Melting Processes:** Understanding the freezing and melting behavior of various substances, such as metals, polymers, and food products. Stefan problem used to model

*Corresponding author

E-mail addresses: sh.pishnamaz@tabrizu.ac.ir (S. Sh. Pishnamaz Mohammadi), ivaz@tabrizu.ac.ir (K. Ivaz)
Academic Editor: Abbas Saadatmandi

how the interface between solid and liquid phases moves over time, helping to optimize processes like casting, welding, and the preservation of perishable goods.

3. **Alloy Solidification:** In metallurgy, controlling the solidification of alloys to achieve the desired properties in the final product. Stefan problem: models the solidification front and predicts the formation of microstructures within the alloy, aiding in the design of processes like continuous casting.

4. **Ice Formation:** In atmospheric chemistry and environmental science, predicting ice formation in clouds, on aircraft surfaces, or in sea ice. Stefan problem helps to model how ice forms and grows under varying environmental conditions, contributing to better weather prediction and climate models.

5. **Pharmaceuticals:** In the development of freeze-drying processes for pharmaceuticals. Stefan problem: models the sublimation front during the freeze-drying process, helping to optimize conditions for the stability and effectiveness of the final product.

6. **Geological Processes:** Understanding the formation of geological features such as permafrost and lava solidification. Stefan problem: models the heat exchange and phase change in geological stuffs, providing insights into the timescales and conditions under which these processes occur.

Each of these applications benefits from the Stefan problem's ability to model the dynamic nature of phase change boundaries, leading to improved control and optimization of industrial and natural processes.

Phase transitions are found in several related processes in physics, chemistry, natural sciences, and engineering: almost every industrial product involves solidification at some stage. Chemical examples include metal casting, steel annealing, crystal growth, thermal welding, soil freezing, surface water freezing and thawing, food preservation, etc. An example is the ice melting problem, which was first treated by Stefan [1] and has since been widely called Stefan problems [2–7]. Stefan's simple one-phase fuzzy model is reviewed in [8]. Topics related to one-phase Stefan problems, including the non-classical heat equation and integral boundary conditions, are discussed in [9–11], and the numerical methods used in [12–14]. We are looking for a free border problem in such issues.

Consider the following problem:

$$v_t - v_{xx} = -F(v_x(0, t)), \quad \gamma(t) \geq x \geq 0, \quad T \geq t \geq 0, \quad (1)$$

$$v(0, t) + \alpha v_x(0, t) = f_1(t), \quad T \geq t \geq 0, \quad (2)$$

$$v(\gamma(t), t) = 0, \quad T \geq t \geq 0, \quad (3)$$

$$v(x, 0) = h_1(x) \geq 0, \quad b \geq t \geq 0, \quad (4)$$

$$v_x(\gamma(t), t) = -\dot{\gamma}(t), \quad T \geq t \geq 0 \quad (5)$$

$$\gamma(0) = b, \quad b > 0. \quad (6)$$

In which $\alpha \in \mathbb{R}^+$, $F \in C^1(\mathbb{R}^+)$, $f_1 \in C^0(\mathbb{R}^+)$, $h_1 \in C^1[0, b]$, and $h_1(x) > 0$, $x > 0$, $h_1(b) = 0$ are continuous functions. The function F is called the control function. The diffusion equation with integral conditions has found wide applications in science, especially chemistry and thermoelasticity [12]. In this article, we consider the following problem that involves the integral condition.

$$V_t - V_{xx} = -F(V_x(0, t)), \quad \Gamma(t) \geq x \geq 0, \quad T \geq t \geq 0, \quad (7)$$

$$V(0, t) + \alpha V_x(0, t) = \int_0^{\Gamma(t)} \phi(x, t) V(x, t) dx + g(t), \quad T \geq t \geq 0, \quad (8)$$

$$V(\Gamma(t), t) = 0, \quad T \geq t \geq 0, \quad (9)$$

$$V(x, 0) = f(x) \geq 0, \quad b \geq t \geq 0, \quad (10)$$

$$V_x(\Gamma(t), t) = -\dot{\Gamma}(t), \quad T \geq t \geq 0, \quad (11)$$

$$\Gamma(0) = b, \quad b > 0. \quad (12)$$

In which $\alpha \in \mathfrak{R}^+$, $F \in C^1(\mathfrak{R}^+)$, $g \in C^0(\mathfrak{R}^+)$, $f_1 \in C^1[0, b]$, and $f_1(b) = 0$.

The general structure of the article is as follows. First, the explicit numerical solution based on finite differences for (7-12) is discussed. In the second step, the convergence of the method is checked, and finally, the numerical results are presented as examples.

2 Numerical review and convergence

In the continuation of the discussion, the number of intervals between the fixed boundary $x = 0$ and the moving boundary $x = \Gamma(t)$ will be considered equal to N . The moving boundary is placed in the N th grid. By tracking particular grid lines, as opposed to constant x , and differentiating with respect to time t , the following expression was obtained for i th grid point,

$$\left[\frac{\partial V}{\partial t} \right]_i = \left[\frac{\partial V}{\partial x} \right]_t \left[\frac{dx}{dt} \right]_i + \left[\frac{\partial V}{\partial t} \right]_x, \quad (13)$$

and was also assumed that the node x_i is moved by the expression

$$\frac{dx_i}{dt} = \frac{x_i}{\Gamma(t)} \times \frac{d\Gamma}{dt}. \quad (14)$$

In which the suffices t, i , and x are to be kept constant during the differentiation processes and omitted for clarity below. Thus, in the dimensionless model problem, the heat conduction Equation (7) takes the form

$$\frac{\partial V}{\partial t} = \frac{\partial^2 V}{\partial x^2} + \frac{x_i \dot{\Gamma}(t)}{\Gamma(t)} \frac{\partial V}{\partial x} - F(V(0, t)), \quad 0 \leq x \leq \Gamma(t), \quad 0 \leq t \leq T. \quad (15)$$

One explicit finite difference representation of Equation (15) is

$$v_{i,j+1} = \mathbf{r}v_{i-1,j} + \left(1 - 2\mathbf{r} - \frac{\mathbf{k}x_i \dot{\gamma}_j}{\mathbf{h}\gamma_j}\right)v_{i,j} + \left(\mathbf{r} + \frac{\mathbf{k}x_i \dot{\gamma}_j}{\mathbf{h}\gamma_j}\right)v_{i+1,j} - \mathbf{k}F(v_{0,j}), \quad i = 1, 2, \dots, N-1, \quad j = 1, 2, \dots, \quad (16)$$

with a truncation error of $O(k) + O(h^2)$. To approximate the integral on the second side of Equation (8), we use the composite Simpson rule,

$$\frac{\mathbf{h}}{3} \left[v_{0,j} \varphi_{0,j} + 4 \sum_{l=1}^n v_{2l-1,j} \varphi_{2l-1,j} + 2 \sum_{l=1}^n v_{2l-2,j} \varphi_{2l-2,j} + v_{2n,j} \varphi_{2n,j} \right], \quad (17)$$

$$j = 1, 2, \dots, N = 2n.$$

From the boundary condition (9), $v_{N,j} = 0$, it can be concluded that $v_{N,j} \varphi_{N,j} = 0$. So for the boundary condition (9) at $x = 0$, using the central difference, we can express:

$$v_{1,j} + \alpha \frac{v_{2,j} - v_{0,j}}{2\mathbf{h}} = \frac{\mathbf{h}}{3} \left[v_{0,j} \varphi_{0,j} + 4 \sum_{l=1}^n v_{2l-1,j} \varphi_{2l-1,j} + 2 \sum_{l=1}^n v_{2l-2,j} \varphi_{2l-2,j} \right] + g(t_j), \quad j = 1, 2, \dots, N = 2k. \quad (18)$$

Note: In this article, the following approximations are used:

$$v_{i,j} \approx V(x_i, t_j),$$

$$\gamma_j \approx \Gamma(t_j), t_j = j\mathbf{k},$$

$$\mathbf{k} = \mathbf{T}/\mathbf{M},$$

$$x_i = i\mathbf{h}, (\mathbf{h} \approx \Delta x),$$

$$\mathbf{r} = \mathbf{k}/\mathbf{h}^2.$$

For Stefan's condition (11), we can state

$$\gamma_{j+1} = \gamma_j - \frac{\mathbf{k}}{2\mathbf{h}} (3v_{N,j} - 4v_{N-1,j} + v_{N-2,j}), j = 1, 2, \dots, \quad (19)$$

and for the boundary conditions (9), (10) and (12) we can state,

$$v_{i,j} = 0, i = N, j = 1, 2, \dots, v_{i,0} = f_i, i = 1, 2, \dots, \gamma_0 = b. \quad (20)$$

3 Convergence and stability

One of the most important discussions of numerical methods is to prove the convergence of that method. Therefore, first, we check the convergence of the method used in this paper. By choosing the mesh points, $v_{i,j} = V_{i,j} - \mathbf{e}_{i,j}$, and using the Taylor expansion, we can obtain from (16).

$$\begin{aligned} \mathbf{e}_{i,j+1} = & \mathbf{r}\mathbf{e}_{i-1,j} + \left(1 - 2\mathbf{r} - \frac{\mathbf{k}x_i\dot{\gamma}_j}{\mathbf{h}\gamma_j}\right) \mathbf{e}_{i,j} + \left(\mathbf{r} + \frac{\mathbf{k}x_i\dot{\gamma}_j}{\mathbf{h}\gamma_j}\right) \mathbf{e}_{i+1,j} - \mathbf{k}\mathbf{e}_{0,j}F'(\Theta) \\ & + \mathbf{k}\left[\left(\frac{\partial V}{\partial t}\right)(x_i, t_j + \Theta_1\mathbf{k}) - \left(\frac{\partial^2 V}{\partial x^2}\right)(x_i + \Theta_2\mathbf{h}, t_j)\right. \\ & \left. - \frac{x_i\dot{\gamma}_j}{\gamma_j} \left(\frac{\partial V}{\partial x}\right)(x_i + \Theta_3\mathbf{h}, t_j) + F(V_{0,j})\right]. \end{aligned} \quad (21)$$

In which, $-1 < \Theta_2 < 1$, $0 < \Theta_1, \Theta_3 < 1$, and Θ is between $V_{0,j} - \mathbf{e}_{0,j}$ and $V_{0,j}$. If $\mathbf{k} < \frac{\mathbf{h}^2\gamma_j}{2\gamma_j + \mathbf{h}x_i\dot{\gamma}_j}$, for each step $\mathbf{h}, \mathbf{k}, i = 1, \dots, N-1, j = 0, 1, \dots$, we can write

$$|\mathbf{e}_{i,j+1}| \leq \mathbf{r}|\mathbf{e}_{i-1,j}| + \left[1 - 2\mathbf{r} - \frac{\mathbf{k}x_i\dot{\gamma}_j}{\mathbf{h}\gamma_j}\right] |\mathbf{e}_{i,j}| + \left[\mathbf{r} + \frac{\mathbf{k}x_i\dot{\gamma}_j}{\mathbf{h}\gamma_j}\right] |\mathbf{e}_{i+1,j}| + \mathbf{k}M_1 + \mathbf{k}N_1. \quad (22)$$

Suppose that the largest error value $|\mathbf{e}_{i,j}|$ during the time row j is \mathbf{ER}_j . Also, the largest value of brackets in (22) for all values of i, j and \mathbf{h}, \mathbf{k} is M_1 , and the largest absolute value of $|\mathbf{e}_{0,j}F'(\Theta)|$ is N_1 . So

$$\begin{aligned} \mathbf{ER}_{j+1} & \leq \mathbf{ER}_j + \mathbf{k}(M_1 + N_1) \\ & \leq (\mathbf{ER}_{j-1} + \mathbf{k}(M_1 + N_1)) + \mathbf{k}(M_1 + N_1) \\ & = \mathbf{ER}_{j-1} + 2\mathbf{k}(M_1 + N_1) \\ & \leq \dots \leq \mathbf{ER}_0 + j\mathbf{k}(M_1 + N_1). \end{aligned} \quad (23)$$

It is obtained from (23), $\mathbf{ER}_j \leq \mathbf{ER}_0 + j\mathbf{k}(M_1 + N_1)$. Because the initial values of v and V are equal, therefore $\mathbf{ER}_0 = 0$. When $\mathbf{h} \rightarrow 0$, $\mathbf{k} = \mathbf{r}\mathbf{h}^2$ is also zero and M_1 tends to

$$\left(\frac{\partial V}{\partial t} - \frac{\partial^2 V}{\partial x^2} - \frac{x_i\dot{\gamma}_j}{\Gamma_j} \frac{\partial V}{\partial x} + F(V(0, t))\right)_{i,j}. \quad (24)$$

We know that V, Γ is a solution to Equation (15), and M_1 is bounded, so \mathbf{ER}_j is zero. From $|V_{i,j} - v_{i,j}| \leq \mathbf{ER}_j, j = 0, 1, \dots$. It can be concluded that when $\mathbf{k} < \frac{\mathbf{h}^2\gamma_j}{2\gamma_j + \mathbf{h}x_i\dot{\gamma}_j}, i = 1, \dots, N-1, j =$

$0, 1, \dots$ as $\mathbf{h} \rightarrow 0$, v converges to V .

To prove the convergence γ_j to Γ_j using the relation (19) and assumption $\gamma_{j+1} = \Gamma_{j+1} - \mathbf{e}'_{j+1}$, $\gamma_j = \Gamma_j - \mathbf{e}'_j$, we have

$$\Gamma_{j+1} - \mathbf{e}'_{j+1} = \Gamma_j - \mathbf{e}'_j - \frac{\mathbf{k}}{2\mathbf{h}} (3V_{N,j} - 3\mathbf{e}_{N,j} - 4V_{N-1,j} + 4\mathbf{e}_{N-1,j} + V_{N-2,j} - \mathbf{e}_{N-2,j}),$$

$$j = 0, 1, \dots$$

hence

$$\mathbf{e}'_{j+1} = \mathbf{e}'_j + \Gamma_{j+1} - \Gamma_j - \frac{\mathbf{k}}{2\mathbf{h}} (3V_{N,j} - 3\mathbf{e}_{N,j} - 4V_{N-1,j} + 4\mathbf{e}_{N-1,j} + V_{N-2,j} - \mathbf{e}_{N-2,j}),$$

$$j = 0, 1, \dots \quad (25)$$

Using the Taylor expansion, we obtain:

$$\mathbf{e}'_{j+1} = \mathbf{e}'_j + \mathbf{k}\Gamma'(t_j + \Theta_5\mathbf{k}) - \frac{3\mathbf{k}}{2\mathbf{h}}\mathbf{e}_{N,j} + \frac{2\mathbf{k}}{\mathbf{h}}\mathbf{e}_{N-1,j} - \frac{\mathbf{k}}{2\mathbf{h}}\mathbf{e}_{N-2,j}$$

$$- \frac{\mathbf{k}}{2\mathbf{h}} (3V_{N,j} - 4V_{N,j} + 4\mathbf{h} \left(\frac{\partial V}{\partial x}\right) (x_N - \Theta_6\mathbf{h}, t_j) + V_{N,j} - 2\mathbf{h} \left(\frac{\partial V}{\partial x}\right) (x_N - \Theta_7\mathbf{h}, t_j)). \quad (26)$$

In relation (26), since $0 < \Theta_i\mathbf{h} < \mathbf{h}$, $i = 6, 7$, so for sufficiently small step size h , $\Theta_6 \cong \Theta_7$ and we can write

$$\mathbf{e}'_{j+1} = \mathbf{e}'_j + \mathbf{k} \left[\Gamma'(t_j + \Theta_5\mathbf{k}) + \left(\frac{\partial V}{\partial x}\right) (x_N - \Theta_6\mathbf{h}, t_j) \right]$$

$$- \frac{3\mathbf{k}}{2\mathbf{h}}\mathbf{e}_{N,j} + \frac{2\mathbf{k}}{\mathbf{h}}\mathbf{e}_{N-1,j} - \frac{\mathbf{k}}{2\mathbf{h}}\mathbf{e}_{N-2,j},$$

then

$$|\mathbf{e}'_{j+1}| \leq |\mathbf{e}'_j| + \mathbf{k} \left| \left[\Gamma'(t_j + \Theta_5\mathbf{k}) + \left(\frac{\partial V}{\partial x}\right) (x_N - \Theta_6\mathbf{h}, t_j) \right] \right| + \frac{3\mathbf{k}}{2\mathbf{h}} |\mathbf{e}_{N,j}|$$

$$+ \frac{2\mathbf{k}}{\mathbf{h}} |\mathbf{e}_{N-1,j}| + \frac{\mathbf{k}}{2\mathbf{h}} |\mathbf{e}_{N-2,j}|. \quad (27)$$

Assuming Π is the largest value inside the bracket in (27), then

$$|\mathbf{e}'_{j+1}| \leq |\mathbf{e}'_j| + \mathbf{k}\Pi + \left(\frac{3\mathbf{k}}{2\mathbf{h}} + \frac{2\mathbf{k}}{\mathbf{h}} + \frac{\mathbf{k}}{\mathbf{h}}\right) \mathbf{E}_j = |\mathbf{e}'_j| + \mathbf{k}\Pi + \left(\frac{4\mathbf{k}}{\mathbf{h}}\right) \mathbf{E}_j$$

$$\leq |\mathbf{e}'_{j-1}| + 2\mathbf{k}\Pi + \left(\frac{4\mathbf{k}}{\mathbf{h}}\right) (\mathbf{E}_{j-1}) \quad (28)$$

$$\leq \dots \leq |\mathbf{e}'_0| + j\mathbf{k}\Pi + \left(\frac{4\mathbf{k}}{\mathbf{h}}\right) \mathbf{E}\mathbf{R}_0,$$

Since the initial values of (γ, v) and (Γ, V) are the same, so $\mathbf{e}'_0 = 0$ and $\mathbf{E}\mathbf{R}_0 = 0$.

When $\mathbf{k} \rightarrow 0$ then Π will approach $\left(\dot{\Gamma}(t) + \frac{\partial V}{\partial x} \Big|_{x=\Gamma(t)}\right)_j$. Since (Γ, V) is a solution to problem (7-12), when $\mathbf{h} \rightarrow 0$, $\mathbf{k} \rightarrow 0$ then $\Pi \rightarrow 0$ therefore $|\mathbf{e}'_{j+1}| \rightarrow 0$. By $|\Gamma_{j+1} - \gamma_{j+1}| \leq \mathbf{e}'_{j+1}$, so γ converges to Γ .

3.1 Stability

We investigate the stability of the difference equation (16) in the case $F(v) = v$ by Von Neumann's method. We consider the following difference equation:

$$v_{p,q+1} = \mathbf{r}v_{p-1,q} + \left(1 - 2\mathbf{r} - \frac{\mathbf{k}x_p\dot{\gamma}_q}{\mathbf{h}\gamma_q}\right) v_{p,q} + \left(\mathbf{r} + \frac{\mathbf{k}x_p\dot{\gamma}_j}{\mathbf{h}\gamma_q}\right) v_{p+1,q}$$

$$- \mathbf{k}v_{0,q}, \quad (29)$$

Substitution of $v_{p,q} = e^{i\beta_n p \mathbf{h} \zeta^q}$ into the difference equation (29) shows that

$$e^{i\beta_n p \mathbf{h} \zeta^{q+1}} = \mathbf{r}e^{i\beta_n (p-1) \mathbf{h} \zeta^q} + \left(1 - 2\mathbf{r} - \frac{\mathbf{k}x_p\dot{\gamma}_q}{\mathbf{h}\gamma_q}\right) e^{i\beta_n p \mathbf{h} \zeta^q}$$

$$+ \left(\mathbf{r} + \frac{\mathbf{k}x_p\dot{\gamma}_j}{\mathbf{h}\gamma_q}\right) e^{i\beta_n (p+1) \mathbf{h} \zeta^q} - \mathbf{k}\zeta^q, \quad (30)$$

where $\mathbf{r} = \mathbf{k}/\mathbf{h}^2$, $\beta_n = \frac{n\pi}{N\mathbf{h}}$ and $N\mathbf{h} = b$. Devision by $e^{i\beta_n p \mathbf{h} \xi^q}$ leads to

$$\xi = \mathbf{r}e^{-i\beta_n \mathbf{h}} + \left(1 - 2\mathbf{r} - \frac{\mathbf{k}x_p \dot{\gamma}_q}{\mathbf{h}\gamma_q}\right) + \left(\mathbf{r} + \frac{\mathbf{k}x_p \dot{\gamma}_j}{\mathbf{h}\gamma_q}\right) e^{i\beta_n \mathbf{h}} - \mathbf{k}e^{-i\beta_n p \mathbf{h}}. \quad (31)$$

Hence

$$|\xi| \leq \left| \mathbf{r}e^{-i\beta_n \mathbf{h}} + \left(1 - 2\mathbf{r} - \frac{\mathbf{k}x_p \dot{\gamma}_q}{\mathbf{h}\gamma_q}\right) + \left(\mathbf{r} + \frac{\mathbf{k}x_p \dot{\gamma}_j}{\mathbf{h}\gamma_q}\right) e^{i\beta_n \mathbf{h}} \right| + |\mathbf{k}e^{-i\beta_n p \mathbf{h}}|, \quad (32)$$

therefore

$$|\xi| \leq \mathbf{r} + \left|1 - 2\mathbf{r} - \frac{\mathbf{k}x_p \dot{\gamma}_q}{\mathbf{h}\gamma_q}\right| + \mathbf{r} + \frac{\mathbf{k}x_p \dot{\gamma}_j}{\mathbf{h}\gamma_q} \mathbf{k}, \quad p = 1, 2, \dots, N-1, q = 1, 2, \dots, \quad (33)$$

satisfies the Von Neumann condition for stability if $\mathbf{k} \leq (1 - 2\mathbf{r}) \frac{\mathbf{h}\gamma_q}{x_p \dot{\gamma}_q}$.

4 Numerical results

Finally, two examples are considered to show the closeness of the solutions obtained from the method mentioned in the article to the exact solutions. All calculations were performed on a AMD A10 2.0 GHz CPU and using Matlab software version 2020b.

Example 4.1. Consider the one-phase, diffusion-reaction and non-classical heat equation following

$$\begin{cases} V_t - V_{xx} = \exp(2t) + 1, & \gamma(t) \geq x \geq 0, T \geq t \geq 0, \\ V(0, t) + 0.5V_x(0, t) = \int_0^{\Gamma(t)} 2\exp(-t)V(x, t)dx - \frac{1}{6}\exp(2t), & T \geq t \geq 0, \\ V(\Gamma(t), t) = 0, & T \geq t \geq 0, \\ V_x(\Gamma(t), t) = -\dot{\Gamma}(t), & T \geq t \geq 0, \\ V(x, 0) = \frac{1}{2}(1 - x^2), & \gamma(t) \geq x \geq 0, \\ \Gamma(0) = 1. \end{cases}$$

The exact solution is

$$V(x, t) = \frac{1}{2}(\exp(2t) - x^2), \quad \Gamma(t) = \exp(t).$$

(**Discrete form of Example 4.1**) The explicit finite difference of [Example 4.1](#) is as follows:

$$\begin{aligned} -rv_{i-1,j+1} + (2 - 2r)v_{i,j+1} - rv_{i+1,j+1} &= \left(r - \frac{kx_i \dot{\gamma}_j}{h\gamma_j}\right) v_{i-1,j} + (2 - 2r)v_{i,j} \\ &+ \left(r + \frac{kx_i \dot{\gamma}_j}{h\gamma_j}\right) v_{i+1,j} + 2k(\exp(2t) + 1), \quad j = 0, 1, \dots, i = 2, \dots, N-1. \end{aligned}$$

[Tables 1](#) and [2](#) display, respectively, the numerical results for the temperature distribution and the interface movement at a final time of $t_f = 0.5$. It is observed that all the results are in good agreement with the exact solution, and exhibit the expected convergence as the mesh size is refined. The interface predictions shown in [Table 3](#) are also in good agreement with the exact interface location at some internal points between the initial time, $t_0 = 0$ and the final time, $t_f = 0.5$. For example, at $t_f = 0.5$ the percentage error decreases from $0.2 \times 10^{-2}\%$ ($N = 40$)

to $0.8 \times 10^{-3}\%$ ($N = 320$). Figure 1 compares the exact temperature distribution with the numerical approximation. Figure 2 illustrates the absolute error graph of this example. Figure 3 compares the numerical moving boundary with the exact moving boundary.

Table 1: Variable space grid: Values of the temperature distribution as predicted by the numerical (explicit finite-difference) and exact solutions at a final time of $t_f = 0.5$.

x/s	Numerical solution				Exact solution
	$N = 40$	$N = 80$	$N = 160$	$N = 320$	
0.0	1.3640	1.3616	1.3604	1.3598	1.3591
0.1	1.3479	1.3468	1.3462	1.3459	1.3456
0.2	1.3053	1.3050	1.3049	1.3048	1.3048
0.3	1.2360	1.2364	1.2366	1.2367	1.2369
0.4	1.1399	1.1408	1.1412	1.1415	1.1417
0.5	1.0170	1.0182	1.0188	1.0191	1.0195
0.6	0.8673	0.8686	0.8692	0.8695	0.8700
0.7	0.6907	0.6919	0.6925	0.6928	0.6934
0.8	0.4873	0.4883	0.4888	0.4890	0.4896
0.9	0.2570	0.2576	0.2579	0.2581	0.2586
1.0	0	0	0	0	0

Table 2: Variable space grid: Values of the location and speed of the moving interface as predicted by the numerical (explicit finite-difference) and exact solutions at a final time of $t_f = 0.5$.

N	Numerical solution			
	γ_j	Error	$\dot{\gamma}_j$	Error
40	1.6467	0.0020	1.6423	0.0064
80	1.6477	0.0010	1.6455	0.0032
160	1.6482	0.0005	1.6471	0.0016
320	1.6485	0.0003	1.6479	0.0008

Table 3: Location of the moving boundary.

t	Numerical solution				Exact values of $\gamma(t_j)$
	$N = 40$	$N = 80$	$N = 160$	$N = 320$	
0.1	1.1050	1.1051	1.1051	1.1051	1.1052
0.2	1.2209	1.2211	1.2213	1.2213	1.2214
0.3	1.3489	1.3494	1.3496	1.3497	1.3499
0.4	1.4904	1.4911	1.4915	1.4916	1.4918
0.5	1.6467	1.6477	1.6482	1.6485	1.6487

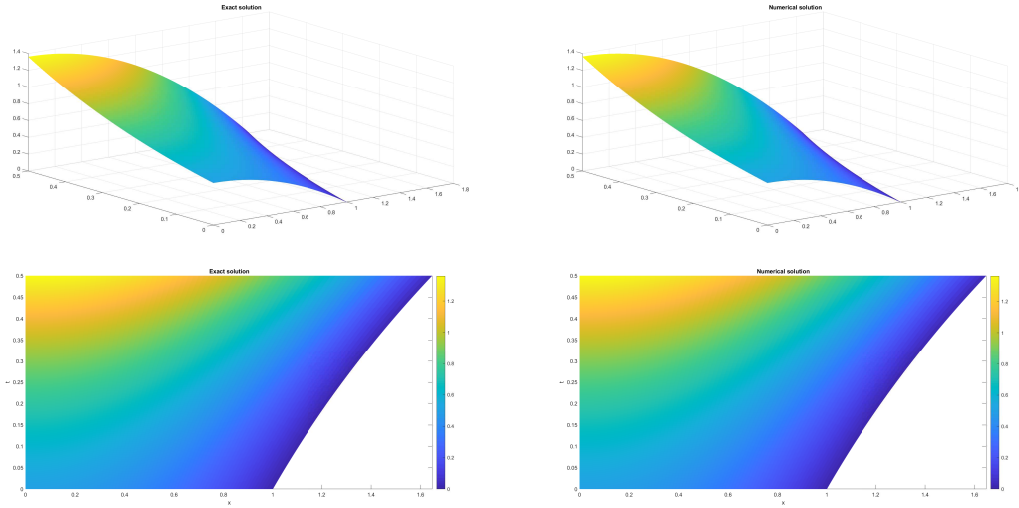


Figure 1: Comparison of the exact temperature distribution of [Example 4.1](#) with the numerical approximation. The right pictures are the exact solution and left pictures are the numerical solution.

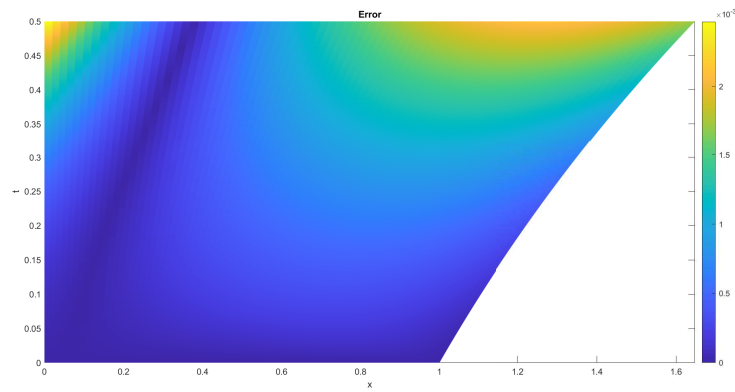


Figure 2: Absolute error graph of [Example 4.1](#).

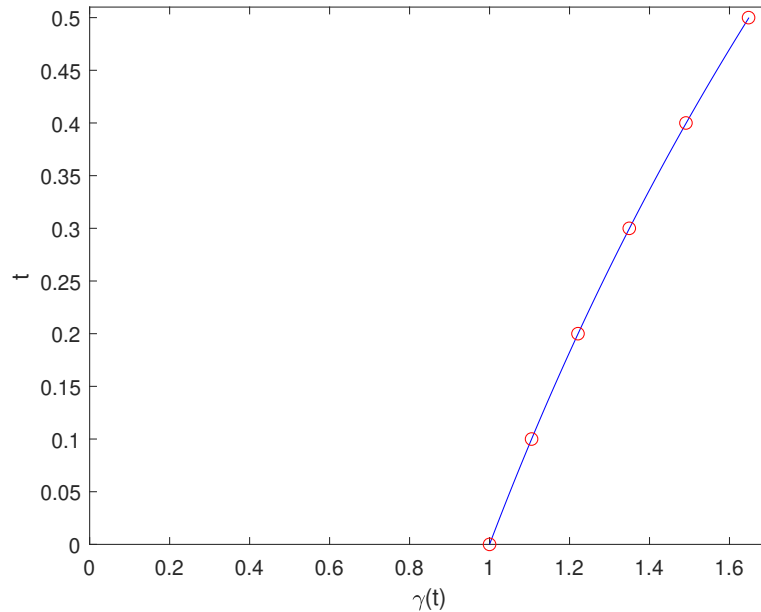


Figure 3: Comparison of the numerical moving boundary with the exact moving boundary of Example 4.1.

Example 4.2.

$$\left\{ \begin{array}{ll} V_t - V_{xx} = 1, & \gamma(t) \geq x \geq 0, 1/2 \geq t \geq 0, \\ V(0, t) + \alpha V_x(0, t) = \int_0^{\Gamma(t)} \psi(x, t) V(x, t) dx + g(t), & 1/2 \geq t \geq 0, \\ V(\Gamma(t), t) = 0, & 1/2 \geq t \geq 0, \\ V_x(\Gamma(t), t) = -\dot{\Gamma}(t), & 1/2 \geq t \geq 0, \\ V(x, 0) = 1/2 - x, & \gamma(t) \geq x \geq 0. \\ \Gamma(0) = 1/2. & \end{array} \right.$$

In which $\psi(x, t) = x$, $g(t) = t - \frac{1}{6}(t + 1/2)^3$, $\alpha = 1/2$, and the exact solution is given by $V(x, t) = -x + t + 1/2$, $\Gamma(t) = t + 1/2$.

Tables 4 and 5 display, respectively, the numerical results for the temperature distribution and the interface movement at a final time of $t_f = 0.5$. It is observed that all the results are in good agreement with the exact solution, and exhibit the expected convergence as the mesh size is refined. The interface predictions shown in Table 6 are also in good agreement with the exact interface location at some internal points between the initial time, $t_0 = 0$ and the final time, $t_f = 0.5$. Figure 4 compares the exact temperature distribution with the numerical approximation. Figure 5 compares the numerical moving boundary with the exact moving boundary. Figure 6 illustrates the absolute error graph of this example.

Table 4: Variable space grid: Values of the location and speed of the moving interface as predicted by the numerical (explicit finite-difference) and exact solutions at a final time of $t_f = 0.5$.

x/s	Numerical solution				Exact solution(Γ)
	$N = 10$	$N = 20$	$N = 40$	$N = 80$	
0.0	1.000000000008199	1.000000000008275	1.000000000008302	1.000000000008254	1.000000000000000
0.1	0.900000000006754	0.900000000006816	0.900000000006835	0.900000000006796	0.900000499999672
0.2	0.800000000005511	0.800000000005563	0.800000000005580	0.800000000005547	0.800000999999345
0.3	0.700000000004427	0.700000000004478	0.700000000004490	0.700000000004462	0.700001499999017
0.4	0.600000000003464	0.600000000003516	0.600000000003530	0.600000000003507	0.600001999998690
0.5	0.500000000002589	0.500000000002649	0.500000000002665	0.500000000002649	0.500002499998362
0.6	0.400000000001882	0.400000000001927	0.400000000001931	0.400000000001917	0.400002999998035
0.7	0.300000000001308	0.300000000001345	0.300000000001341	0.300000000001329	0.300003499997707
0.8	0.200000000000842	0.200000000000864	0.200000000000858	0.200000000000849	0.200003999997380
0.9	0.100000000000412	0.100000000000420	0.100000000000417	0.100000000000413	0.100004499997052
1.0	0	0	0	0	0

Table 5: Variable space grid: Values of the location and speed of the moving interface as predicted by the numerical (explicit finite-difference) and exact solutions at a final time of $t_f = 0.5$.

N	Numerical solution			
	γ_j	Error	$\dot{\gamma}_j$	Error
10	1.000000000000500	0.000000000000500	1.000000000000546	0.000000000000546
20	1.000000000000500	0.000000000000500	1.000000000000502	0.000000000000502
40	1.000000000000500	0.000000000000500	1.000000000000514	0.000000000000514
80	1.000000000000500	0.000000000000500	1.000000000000514	0.000000000000514

Table 6: Location of the moving boundary.

t	Numerical solution				Exact values of $\gamma(t_j)$
	$N = 40$	$N = 80$	$N = 160$	$N = 320$	
0.1	0.600000000000655	0.600000000000655	0.600000000000655	0.600000000000655	0.600000000000000
0.2	0.700000000001310	0.700000000001310	0.700000000001310	0.700000000001310	0.700000000000000
0.3	0.800000000001965	0.800000000001965	0.800000000001965	0.800000000001965	0.800000000000000
0.4	0.900000000002620	0.900000000002620	0.900000000002620	0.900000000002620	0.900000000000000
0.5	1.000000000003276	1.000000000003276	1.000000000003276	1.000000000003276	1.000000000000000

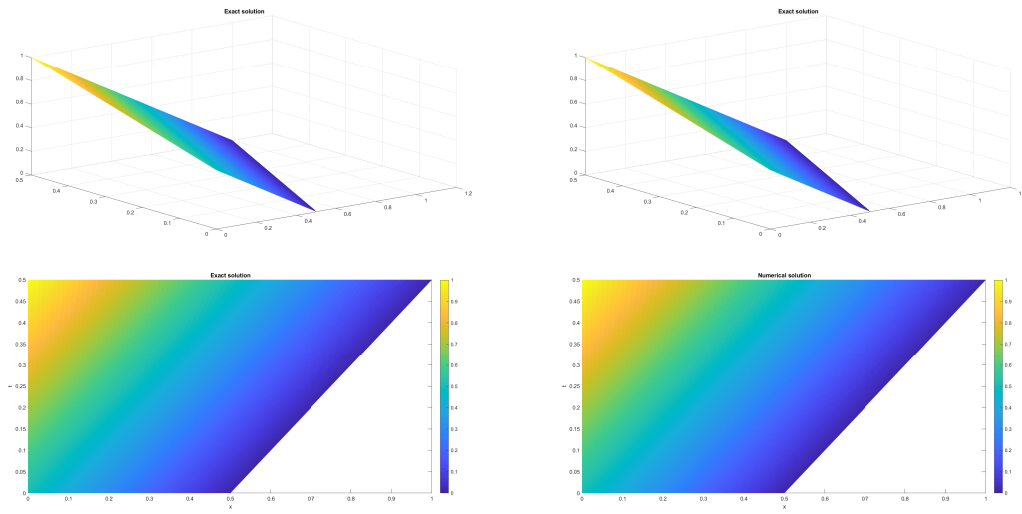


Figure 4: Comparison of the exact temperature distribution of [Example 4.2](#) with the numerical approximation. The right pictures show the exact solution and left pictures show the numerical solution.

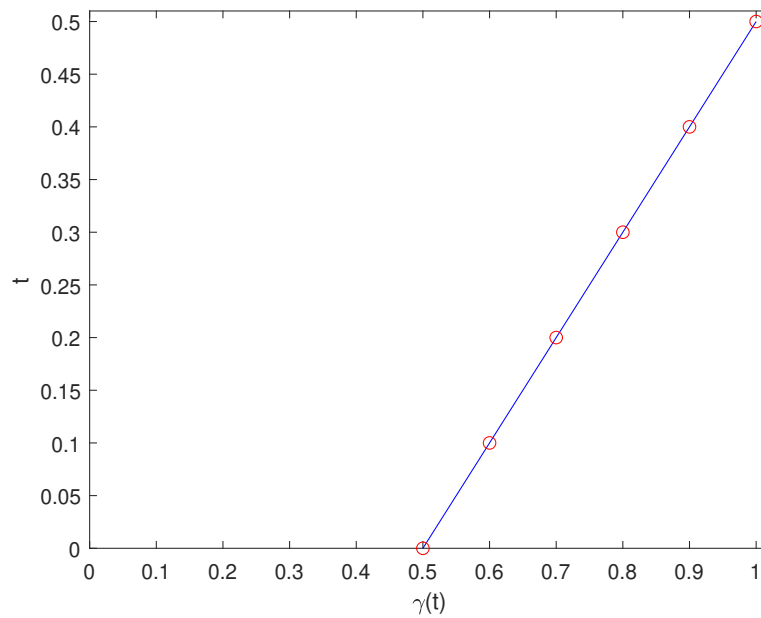


Figure 5: Comparison of the numerical moving boundary with the exact moving boundary of [Example 4.2](#).

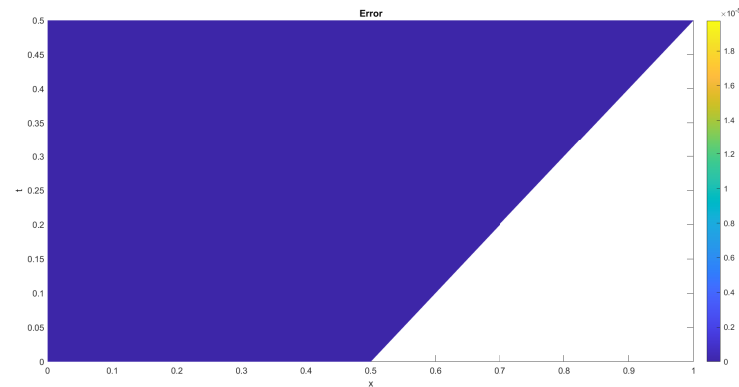


Figure 6: Absolute error graph for Example 4.2.

5 Concluding remarks

This paper has presented a detailed examination of numerical method applied to one-phase Stefan problems, including the non-classical heat equation and integral boundary conditions. The results underscore the importance of choosing suitable numerical schemes to accurately model phase change phenomena, which is critical for applications in fields such as materials science, cryogenics, and geophysics. Our study demonstrates the effectiveness of finite difference in capturing the dynamic behavior of the moving boundary characteristic of the Stefan problem.

Conflicts of Interest. The authors declare that they have no conflicts of interest regarding the publication of this article.

References

- [1] J. Stefan, Ueber die theorie der eisbildung, insbesondere über die eisbildung im polarmeere, *Ann. Phys.* **278** (1891) 269–286, <https://doi.org/10.1002/andp.18912780206>.
- [2] V. Alexiades, *Mathematical Modeling of Melting and Freezing Processes*, New York, 2018.
- [3] B. Babayar-Razlighi, K. Ivaz, M. R. Mokhtarzadeh and A. N. Badamchizadeh, Newton-product integration for a two-phase Stefan problem with kinetics, *Bull. Iranian Math. Soc.* **38** (2012) 853–868.
- [4] B. Babayar-Razlighi, K. Ivaz and M. R. Mokhtarzadeh, Newton-product integration for a Stefan problem with kinetics, *J. Sci. Islam. Repub. Iran* **22** (2011) 51–61.
- [5] J. R. Cannon and M. Primicerio, Remarks on the one-phase Stefan problem for the heat equation with the flux prescribed on the fixed boundary, *J. Math. Anal. Appl.* **35** (1971) 361–373, [https://doi.org/10.1016/0022-247X\(71\)90223-X](https://doi.org/10.1016/0022-247X(71)90223-X).
- [6] J. Crank, *Free and Moving Boundary Problems*, Oxford, Clarendon press, 1987.

- [7] K. Ivaz and A. Beiranvand, Solving the Stefan problem with kinetics, *Comput. Methods Differ. Equ.* **2** (2014) 37–49.
- [8] K. Ivaz, M. Asadpour Fazlollahi, A. Khastan and J. J. Nieto, Fuzzy one-phase Stefan problem, *Appl. Comput. Math.* **22** (2023) 66–79.
- [9] A. C. Briozzo and D. A. Tarzia, A one-phase Stefan problem for a non-classical heat equation with a heat flux condition on the fixed face, *Appl. Math. Comput.* **182** (2006) 809–819, <https://doi.org/10.1016/j.amc.2006.04.043>.
- [10] A. C. Briozzo and D. A. Tarzia, Existence, uniqueness, and an explicit solution for a one-phase Stefan problem for a nonclassical heat equation, *Int. Series Numer. Mech.* **154** (2006) 117–124.
- [11] A. C. Briozzo and D. A. Tarzia, A Stefan problem for a non-classical heat equation with a convective condition, *Appl. Math. Comput.* **217** (2010) 4051–4060, <https://doi.org/10.1016/j.amc.2010.10.015>.
- [12] J. Martín-Vaquero, A. Queiruga-Dios and A. H. Encinas, Numerical algorithms for diffusion-reaction problems with non-classical conditions, *Appl. Math. Comput.* **218** (2012) 5487–5495, <https://doi.org/10.1016/j.amc.2011.11.037>.
- [13] S. Sh. Pishnamaz Mohammadi and K. Ivaz, Numerical solution of one-phase Stefan problem for the non-classical heat equation with a convective condition, *Comput. Methods Differ. Equ.* **11** (2023) 776–784, <https://doi.org/10.22034/CMDE.2023.54177.2266>.
- [14] S. Kutluay, A. R. Bahadir and A. Özdeş, The numerical solution of one-phase classical Stefan problem, *J. Comput. Appl. Math.* **81** (1997) 135–144.